Time-gating improves the spatial resolution of STED microscopy

Jeffrey R. Moffitt,[1,2,4] Christian Osseforth,[1] and Jens Michaelis[1,3,5]

[1]*Department of Chemistry, Ludwig-Maximilians-Universität München, Butenandtstr 11, 81377 München, Germany*
[2]*Currently with Center for Systems Biology, Harvard University, Cambridge, Massachusetts 02138, USA*
[3]*Center for Integrated Protein Science Munich (CIPS[M]), Butenandtstr 11, 81377 München, Germany*
[4]*lmoffitt@mcb.harvard.edu*
[5]*michaelis@lmu.de*

Abstract: Stimulated-emission depletion (STED) microscopy improves image resolution by encoding additional spatial information in a second stimulated-decay channel with a spatially-varying strength. Here we demonstrate that spatial information is also encoded in the fluorophore lifetime and that this information can be used to improve the spatial resolution of STED microscopy. By solving a kinetic model for emission in the presence of a time-varying STED pulse, we derive the effective resolution as a function of fluorophore lifetime and pulse duration. We find that the best resolution for a given pulse power is achieved with a pulse of infinitesimally short duration; however, the maximum resolution can be restored for pulses of finite duration by time-gating the fluorescence signal. In parallel, we consider time-gating in the presence of a continuous-wave (CW) STED beam and find that time-gating produces theoretically unbounded resolution with finite laser power. In both cases, the cost of this improved resolution is a reduction in the brightness of the final image. We conclude by discussing situations in which time-gated STED microscopy (T-STED) may provide improved microscope performance beyond an increase in resolution.

OCIS codes: (110.0180) Microscopy; (100.6640) Superresolution.

References and links

1. G. Patterson, M. Davidson, S. Manley, and J. Lippincott-Schwartz, "Superresolution imaging using single-molecule localization," Annu. Rev. Phys. Chem. **61**(1), 345–367 (2010).
2. S. W. Hell, "Microscopy and its focal switch," Nat. Methods **6**(1), 24–32 (2009).
3. S. W. Hell, "Toward fluorescence nanoscopy," Nat. Biotechnol. **21**(11), 1347–1355 (2003).
4. J. B. Pawley, S. W. Hell, K. I. Willig, M. Dyba, and V. Westphal, "Nanoscale Resolution with Focused Light: Stimulated Emission Depletion and Other Reversible Saturable Optical Fluorescence Transitions Microscopy Concepts," in *Handbook of Biological Confocal Microscopy* (Springer US, 2006), pp. 571–579.
5. E. Betzig, G. H. Patterson, R. Sougrat, O. W. Lindwasser, S. Olenych, J. S. Bonifacino, M. W. Davidson, J. Lippincott-Schwartz, and H. F. Hess, "Imaging intracellular fluorescent proteins at nanometer resolution," Science **313**(5793), 1642–1645 (2006).
6. S. T. Hess, T. P. Girirajan, and M. D. Mason, "Ultra-high resolution imaging by fluorescence photoactivation localization microscopy," Biophys. J. **91**(11), 4258–4272 (2006).
7. M. J. Rust, M. Bates, and X. Zhuang, "Sub-diffraction-limit imaging by stochastic optical reconstruction microscopy (STORM)," Nat. Methods **3**(10), 793–796 (2006).
8. R. Heintzmann, and C. G. Cremer, "Laterally modulated excitation microscopy: improvement of resolution by using a diffraction grating," J. B. Irving, S. Herbert, S. Jan, S. Katarina, and M. V. Pierre, eds. (SPIE, 1999), pp. 185–196.
9. M. G. Gustafsson, D. A. Agard, and J. W. Sedat, "I5M: 3D widefield light microscopy with better than 100 nm axial resolution," J. Microsc. **195**(1), 10–16 (1999).
10. M. G. Gustafsson, "Nonlinear structured-illumination microscopy: wide-field fluorescence imaging with theoretically unlimited resolution," Proc. Natl. Acad. Sci. U.S.A. **102**(37), 13081–13086 (2005).
11. S. R. Pavani, M. A. Thompson, J. S. Biteen, S. J. Lord, N. Liu, R. J. Twieg, R. Piestun, and W. E. Moerner, "Three-dimensional, single-molecule fluorescence imaging beyond the diffraction limit by using a double-helix point spread function," Proc. Natl. Acad. Sci. U.S.A. **106**(9), 2995–2999 (2009).

#139954 - $15.00 USD Received 21 Dec 2010; revised 10 Feb 2011; accepted 11 Feb 2011; published 17 Feb 2011

12. S. W. Hell, and J. Wichmann, "Breaking the diffraction resolution limit by stimulated emission: stimulated-emission-depletion fluorescence microscopy," Opt. Lett. **19**(11), 780–782 (1994).
13. E. Rittweger, K. Y. Han, S. E. Irvine, C. Eggeling, and S. W. Hell, "STED microscopy reveals crystal colour centres with nanometric resolution," Nat. Photonics **3**(3), 144–147 (2009).
14. B. Huang, M. Bates, and X. W. Zhuang, "Super-resolution fluorescence microscopy," Annu. Rev. Biochem. **78**(1), 993–1016 (2009).
15. J. R. Lakowicz, and B. R. Masters, "Principles of fluorescence spectroscopy," J. Biomed. Opt. **13**(2), 029901 (2008).
16. K. I. Willig, B. Harke, R. Medda, and S. W. Hell, "STED microscopy with continuous wave beams," Nat. Methods **4**(11), 915–918 (2007).
17. M. Leutenegger, C. Eggeling, and S. W. Hell, "Analytical description of STED microscopy performance," Opt. Express **18**(25), 26417–26429 (2010).
18. B. Harke, J. Keller, C. K. Ullal, V. Westphal, A. Schönle, and S. W. Hell, "Resolution scaling in STED microscopy," Opt. Express **16**(6), 4154–4162 (2008).
19. M. Dyba, and S. W. Hell, "Focal spots of size lambda/23 open up far-field fluorescence microscopy at 33 nm axial resolution," Phys. Rev. Lett. **88**(16), 163901 (2002).
20. B. R. Rankin, R. R. Kellner, and S. W. Hell, "Stimulated-emission-depletion microscopy with a multicolor stimulated-Raman-scattering light source," Opt. Lett. **33**(21), 2491–2493 (2008).
21. M. Dyba, and S. W. Hell, "Photostability of a fluorescent marker under pulsed excited-state depletion through stimulated emission," Appl. Opt. **42**(25), 5123–5129 (2003).
22. K. Y. Han, K. I. Willig, E. Rittweger, F. Jelezko, C. Eggeling, and S. W. Hell, "Three-dimensional stimulated emission depletion microscopy of nitrogen-vacancy centers in diamond using continuous-wave light," Nano Lett. **9**(9), 3323–3329 (2009).
23. E. Auksorius, B. R. Boruah, C. Dunsby, P. M. P. Lanigan, G. Kennedy, M. A. A. Neil, and P. M. W. French, "Stimulated emission depletion microscopy with a supercontinuum source and fluorescence lifetime imaging," Opt. Lett. **33**(2), 113–115 (2008).

1. Introduction

In the past 10 years, several new microscopy techniques have demonstrated that far-field optics can be used to achieve nanometer-scale spatial resolution with visible light, breaking the resolution limit original proposed by Abbe [1–4]. This resolution can be achieved with conventional, diffraction-limited point-spread functions (PSF) when single fluorophores are selectively imaged, as in STORM, PALM, and FPALM [5–7], or by engineering the effective PSF to have smaller dimensions through the use of structured illumination [8–10] or detection [11]. Additionally, in a set of techniques known as RESOLFT microscopy [4], an engineered PSF is created by optically pumping fluorescent molecules into non-fluorescent states in a spatially-dependent fashion, decreasing the dimensions of the PSF by constraining the spatial extent of molecules capable of emitting fluorescence.

Of the various RESOLFT techniques, the most commonly utilized is stimulated-emission depletion (STED) microscopy [12]. In this technique, excited fluorophores are exposed to light within their emission spectra, producing emission of the same color as the stimulating beam. By introducing a spatial variation to the intensity of this beam, the strength of the second, stimulated-emission channel can be modulated with respect to spontaneous emission, effectively depleting fluorophores in certain locations while leaving others free to emit spontaneously. For example, by using a STED beam with a central minimum (Fig. 1a) fluorophores towards the exterior of the diffraction-limited-PSF can be selectively silenced. By increasing the intensity of the STED illumination, the depleted region will increase, and the resulting PSF can be theoretically squeezed to arbitrarily small dimensions. (Throughout this Letter, we adopt the convention of judging spatial resolution by the spatial extent of the effective PSF.) Remarkably, STED microscopes based on this principle have achieved spatial resolutions up to ~6 nm starting with a PSF ~30-fold larger [13]. With optical resolution on the 10s of nm scale, STED microscopy has begun to image cellular structures previous accessible only via electron microscopy [14].

The core principle behind the resolution enhancement of STED is the ability to encode spatial information in the strength of a second decay channel. This information is then extracted by selectively discarding photons emitted via the second, stimulated channel from those emitted via spontaneous emission. However, when an excited fluorophore is subject to an additional decay channel, the probability of emitting via spontaneous emission is not the only physical property of the fluorophore that is modified. The lifetime of the excited state

#139954 - $15.00 USD Received 21 Dec 2010; revised 10 Feb 2011; accepted 11 Feb 2011; published 17 Feb 2011

also changes, independent of the choice of decay channel [15]. Thus, spatial information is also encoded in the photon arrival times of the spontaneous emission, and it should be possible to improve the resolution of STED microscopy by extracting this temporal information.

In this Letter, we consider the arrival times of the spontaneous emission from excited fluorophores exposed to a spatially varying stimulating beam. We show that spatial information is encoded in the fluorescent lifetimes of these fluorophores and that photon arrival times can be used to decrease the spatial extent of the effective PSF. We consider situations in which the STED beam is either pulsed or continuous wave (CW), and show that in both situations time-gating the fluorescence emission signal, i.e. discarding photons that arrive before a specific time, increases the spatial resolution of the final image. However, this increase in resolution is accompanied by a reduction in image brightness. We term this technique time-gated STED microscopy (T-STED) and conclude by discussing the potential benefits of this type of measurement.

2. Theory

2.1 Temporal dynamics in a STED measurement

To determine the spatial information encoded in excited fluorophore lifetimes, we consider a set of n_0 excited fluorophores at position r with unstimulated lifetimes of $\tau = 1/k$ in the presence of a stimulating beam with a spatially-varying intensity, $I(r)$. We start by assuming that this stimulating beam is pulsed with finite duration, t_s, immediately following an excitation pulse of much shorter duration, and, in later sections, we generalize these results to CW STED sources [16]. For simplicity, we also assume that vibrational relaxation times are negligible compared to the STED pulse duration or the fluorophore lifetime though this assumption can be relaxed if necessary [17]. Finally, we also neglect alternative decay routes for the excited fluorophores, i.e. triplet states or quenching, as the presence of these processes will only lower the effective number of excited fluorophores not change the temporal dynamics we discuss here. Thus, our analysis begins at $t = 0$ with all fluorophores in the same excited state with the same cross-section for stimulated emission, σ (the cross-section for the related absorption transition [12]).

Under these assumptions the number of excited fluorophores at position r, $n(r,t)$, decays in time as

$$\frac{dn(r,t)}{dt} = -kn(r,t) - \sigma I(r)\left(1-\theta(t-t_s)\right)n(r,t) \tag{1}$$

where $\theta(t-t_s)$, the Heaviside step function, represents the finite duration of the STED pulse. We consider this pulse time-profile to simplify our analysis and allow analytic results; however, more complicated profiles can be considered, e.g. Gaussian profiles, with little effect on the dynamics we discuss here.

As time progresses the number of photons emitted from position r in the stimulated channel, N_S, and the spontaneous channel, N_F, grow as

$$\frac{dN_S(r,t)}{dt} = \sigma I(r)\left(1-\theta(t-t_S)\right)n(r,t), \tag{2}$$

$$\frac{dN_F(r,t)}{dt} = kn(r,t). \tag{3}$$

These expressions can be solved via direct integration, yielding the number of excited fluorophores as a function of time

#139954 - $15.00 USD Received 21 Dec 2010; revised 10 Feb 2011; accepted 11 Feb 2011; published 17 Feb 2011

$$n(r,t) = n_0 \begin{cases} e^{-(k+\sigma I(r))t} & :t \le t_S \\ e^{-\sigma I(r) t_S} e^{-kt} & :t > t_S \end{cases} \tag{4}$$

and the total number of photons in each of the two decay channels emitted during time t

$$N_F(r,t) = n_0 \begin{cases} \dfrac{k}{k+\sigma I(r)}\left(1-e^{-(k+\sigma I(r))t}\right) & t \le t_S \\ \dfrac{k}{k+\sigma I(r)} + \dfrac{\sigma I(r)}{k+\sigma I(r)} e^{-(k+\sigma I(r))t_S} - e^{-\sigma I(r) t_S} e^{-kt} & t > t_S \end{cases} \tag{5}$$

and

$$N_S(r,t) = n_0 \begin{cases} \dfrac{\sigma I(r)}{k+\sigma I(r)}\left(1-e^{-(k+\sigma I(r))t}\right) & t \le t_S \\ \dfrac{\sigma I(r)}{k+\sigma I(r)}\left(1-e^{-(k+\sigma I(r))t_S}\right) & t > t_S \end{cases}. \tag{6}$$

The fraction of excited fluorophores that arrive in each of the two channels from position r is derived from the infinite-time limit, yielding

$$\lim_{t\to\infty} N_F(r,t)/n_0 \equiv \eta_{STED}(r) = \frac{k}{k+\sigma I(r)} + \frac{\sigma I(r)}{k+\sigma I(r)} e^{-(k+\sigma I(r))t_S} \tag{7}$$

and

$$\lim_{t\to\infty} N_S(r,t)/n_0 = \frac{\sigma I(r)}{k+\sigma I(r)}\left(1-e^{-(k+\sigma I(r))t_S}\right). \tag{8}$$

By constructing the final image only from photons emitted via spontaneous emission, i.e. Equation (7), the typical STED microscope exploits the spatial information encoded in the choice of decay channel—the $I(r)$ dependence in Eq. (7)—to improve the spatial resolution. Equation (7) is known as the STED depletion factor, $\eta_{STED}(r)$. However, the presence of a spatial dependence in the exponent of Eq. (5)—the fluorescence lifetime—reveals that the presence of STED light also changes the arrival time of emitted photons, independent of the decay channel, confirming that spatial information is also encoded in the temporal dynamics of the fluorescence signal.

2.2 Spatial dependence of decay channels and arrival times

To illustrate the effects of a spatially varying STED beam on the choice of decay channel and on the photon arrival times, we consider a uniform field of excited fluorophores exposed to a STED beam with an intensity distribution given by the Laguerre-Gaussian, LG_{01},

$$I(r) = \gamma r^2 e^{-2r^2/\omega^2} \tag{9}$$

where ω controls the spatial extent of this beam and γ sets its intensity. γ is related to the total power of the STED beam, P, via $\gamma = 4P/(\pi\omega^4)$.

#139954 - $15.00 USD Received 21 Dec 2010; revised 10 Feb 2011; accepted 11 Feb 2011; published 17 Feb 2011

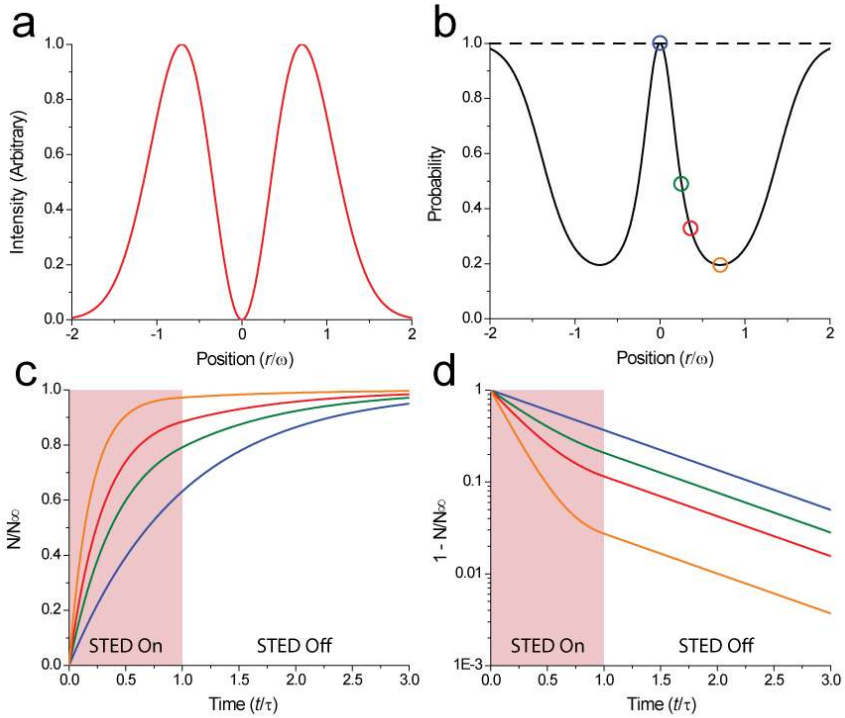

Fig. 1. Fluorophore Lifetimes in the Presence of a Stimulating Beam. (a) The intensity distribution for the stimulating beam. (b) The probability of emitting in the fluorescent channel (solid) when a uniform field of excited fluorophores (dashed) are exposed to a STED beam with $t_S = \tau$ and $S = 23$. (c) The number of fluorophores that have emitted via the spontaneous emission channel as a function of time, normalized by the total number of fluorophores that will emit in this channel ($N_\infty = N_F(t = \infty)$).) The different colors represent different locations along the STED beam corresponding to different probabilities of emitting via spontaneous emission (1, blue; 1/2, green; 1/3, red; 1/5, orange). These positions are circled in panel (b). (d) The fraction of fluorophores that will emit by spontaneous emission but have not yet done so at a given time. All distances are measured in units of spatial parameter of the STED beam, ω, and all times are measured in units of the unstimulated fluorophore lifetime, τ.

For pulsed STED measurements, the ability of the STED beam to deplete excited fluorophores can be characterized with the dimensionless number, the STED strength,

$$S = \sigma\gamma\omega^2 t_S = \sigma\varepsilon. \tag{10}$$

To separate the effect of pulse duration from the total energy contained in the STED beam, it will be useful to redefine the STED strength in terms of the quantity, $\varepsilon = \gamma\omega^2 t_S$, which is proportional to the total energy in the STED pulse. Thus, if the energy in the pulse is constant, varying the pulse duration will not vary the STED strength.

We consider a specific example where the pulse duration is equal to the unstimulated fluorophore lifetime and the STED strength is such that the FWHM of the effective PSF is reduced by a factor of 2. (Later we will derive explicit equations that allow one to determine the specific values for STED strength required for reaching a certain resolution.) Fig. 1b shows that the introduction of this STED beam creates two regions of depleted spontaneous emission in an otherwise uniform field of excited fluorophores. In this case, fluorophores located at the maximum STED intensity, $r_{\max}$, will emit 80% less spontaneous emission. Nevertheless, these fluorophores will still emit ~20% of their fluorescence via this channel, and these photons will ultimately degrade the resolution of the final image.

#139954 - $15.00 USD Received 21 Dec 2010; revised 10 Feb 2011; accepted 11 Feb 2011; published 17 Feb 2011

While the color of these photons cannot be used to discriminate the position of the fluorophore, Figs. 1c and 1d and Eq. (5) reveal that the arrival time of these photons can partially distinguish the fluorophore position. After a time of just 1/10 of the unstimulated lifetime, only 10% of the spontaneous emission from the central minimum of the STED beam ($r=0$; the blue circle in Fig. 1b) has been emitted whereas 40% of the emission from $r_{\max}$ (the orange circle in Fig. 1b) has already arrived. Moreover, by the completion of the STED pulse, only 60% of the emission from $r=0$ while nearly all of the spontaneous emission emitted by fluorophores located at $r_{\max}$ has arrived. Thus, spontaneous emission from fluorophores located at regions of higher STED intensity arrive earlier on average than spontaneous emission from fluorophores exposed to smaller STED intensities, and it should be possible to better distinguish fluorophores located at the center of the STED beam from those located on the edges with time resolved measurements of the spontaneous emission.

2.3 STED resolution for pulses of finite duration

Before we discuss the use of temporal information to improve spatial resolution, it is first useful to determine the effect of pulses of finite duration on the effective PSF of a STED microscope. This section complements recent work by others [17] in which a comprehensive analysis of STED depletion for pulses of finite duration in the presence of vibrational relaxation was conducted. However, for simplicity, we will continue to neglect vibrational relaxation here.

In the typical STED microscope, fluorophores are excited in a Gaussian profile and fluorescence emission is detected in a confocal configuration. This configuration produces a PSF well approximated by

$$PSF_C(r) \sim e^{-4r^2/\omega^2} \tag{11}$$

where ω corresponds to the 1/e waist of the electric field of the excitation beam. For simplicity, we use the same ω for both the STED beam and the confocal PSF though, in practice, the different wavelengths and initial beam sizes for both the excitation and stimulating beams will produce minor differences in ω. The amplitude of the PSF is set by the finite collection and detection efficiency of the optical setup. However, these properties are unaffected by the introduction of a STED beam and, thus, will not affect comparisons between the confocal PSF and the effective STED PSF, so we neglect finite detection efficiency here.

The final effective PSF of a STED microscope is the product of this confocal PSF with the depletion factor provided in Eq. (7) and illustrated in Fig. 1b

$$\begin{aligned} PSF_{STED}(r) &= PSF_C(r)\eta_{STED}(r) \\ &= e^{-4r^2/\omega^2}\left(\frac{k}{k+\sigma I(r)} + \frac{\sigma I(r)}{k+\sigma I(r)} e^{-(k+\sigma I(r))t_S}\right). \end{aligned} \tag{12}$$

To understand the scaling of this PSF, it is useful to introduce dimensionless variables that allow the pulse duration to be varied without changing the total energy in the pulse

$$\alpha = t_S/\tau \text{ and } E(r) = \sigma I(r) t_S. \tag{13}$$

α sets the duration of the STED pulse while $E(r)$ determines the strength of the stimulated emission channel at position *r*, i.e. the energy density of the pulse, $I(r)t_S$, scaled by the cross-section for stimulated emission, σ. With these variables, the STED depletion factor becomes

#139954 - $15.00 USD Received 21 Dec 2010; revised 10 Feb 2011; accepted 11 Feb 2011; published 17 Feb 2011

$$\eta_{STED}(r) = \left(\frac{\alpha}{\alpha + E(r)} + \frac{E(r)}{\alpha + E(r)} e^{-(\alpha + E(r))} \right). \tag{14}$$

The effective PSF for STED microscopy has been calculated previously [18] under the assumption of a STED pulse of negligible duration but fixed energy. Taking the infinitely short STED pulse limit, i.e. $\alpha \to 0$, we recover the previous depletion factor from Eq. (14)

$$\lim_{\alpha \to 0} \eta_{STED}(r) = e^{-\sigma I(r) t_S} = e^{-E(r)}. \tag{15}$$

Comparison of these two expression reveals that for a given pulse energy the depletion produced by a pulse of longer duration is always less than the depletion provided by a pulse of shorter duration. Since less depletion will result in less squeezing of the final PSF, pulses of finite duration will degrade the resolution of the STED microscope. Thus, when vibrational relaxation times are neglected, the best resolution for a given pulse energy will be for the pulse with the shortest duration. (When vibrational relaxation times are included, it has been shown that a small but finite pulse duration produces the optimal resolution [17], and similar results are expected when re-excitation by the STED beam is considered.)

2.4 Time-gated STED (T-STED) resolution

This loss in resolution may initially seem like a limitation to STED pulses of longer durations; however, Eq. (12) ignores the additional spatial information contained in the arrival times of the fluorescent photons (Fig. 1). To exploit this information, we propose that the fluorescence signal used to create the STED image should be time-gated. In other words, only photons arriving after a given time-window will be used to form the final image, as illustrated in Fig. 2a. Assuming a time delay t_G, Eq. (6) provides the depletion factor for a time-gated STED (T-STED) measurement

$$\begin{aligned} \eta_{T-STED}(r; t_G) &= \lim_{t \to \infty} \frac{N_F(t) - N_F(t_G)}{n_0} \\ &= \left(\frac{k}{k + \sigma I(r)} e^{-(k + \sigma I(r)) t_G} + \frac{\sigma I(r)}{k + \sigma I(r)} e^{-(k + \sigma I(r)) t_S} \right). \end{aligned} \tag{16}$$

Since fluorescence decay is a Markov process, arrival times are only modified during the duration of the STED pulse; thus, there is no benefit to time-gates longer than the STED pulse, and we restrict Eq. (16) to $t_G \le t_S$.

Equation (16) reveals that the smallest value of $\eta_{T-STED}(r; t_G)$ and, thus, the smallest effective PSF for a given value of *r* occurs when the time-gate is equal to the STED pulse duration, i.e. $t_G = t_S$, in which case Eq. (16) simplifies significantly

$$\eta_{T-STED}(r; t_G = t_S) = e^{-k t_S} e^{-\sigma I(r) t_S}. \tag{17}$$

Remarkably, Eq. (17) differs from the factor derived in the infinitely short pulse limit, Eq. (15), only in the term $\exp(-k t_S)$. Since this term contains no spatial dependence, it will not affect the spatial extent of the effective PSF; thus, time-gating the fluorescence signal restores the maximum resolution derived in the infinitely-short pulse limit. The additional term, $\exp(-k t_S)$, corresponds to the fraction of fluorophores that decay during the time-gate independent of their position. Rejection of these photons degrades the image brightness without changing the spatial resolution.

#139954 - $15.00 USD Received 21 Dec 2010; revised 10 Feb 2011; accepted 11 Feb 2011; published 17 Feb 2011

Figure 2b plots the factors $\eta_{STED}(r)$ and $\eta_{T-STED}(r;t_G=t_S)$ for the example considered in Fig. 1. By applying a time-gate equal to the STED pulse duration, the 'depleted' region observed in Fig. 1b (black) can be significantly increased (red, dashed). To better compare the increase in the depletion region, Fig. 2b also plots this depletion factor without the $\exp(-kt_S)$ prefactor. For this particular example, time-gating lowers the amount of accepted spontaneous emission nearly 40-fold from fluorophores located at $r_{\max}$. This additional rejection results in a tighter effective PSF, as illustrated in Fig. 2c. The 2-fold improvement in resolution afforded by the depletion of the spontaneous decay channel is increased to 2.5-fold simply by rejecting the spontaneous emission that arrives during the duration of the STED pulse.

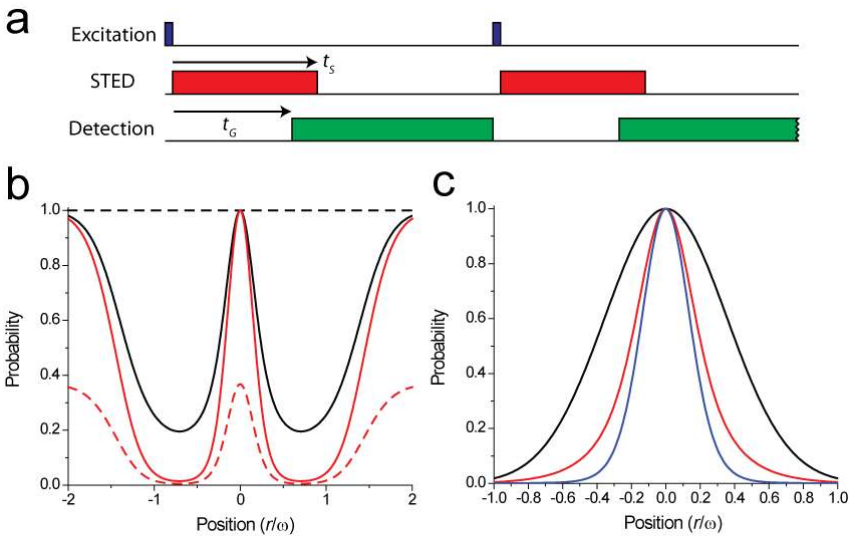

Fig. 2. Improving Spatial Resolution with Time-Gating. (a) Timing diagram for pulsed STED with time-gated detection. Immediately following an excitation pulse of negligible duration (blue), a STED pulse of duration t_S begins (red). The final image is created from the spontaneous emission that arrives during a time window starting t_G after the completion of one excitation pulse and lasting until the beginning of the next (green). (b) The probability of emitting via normal fluorescence as a function of position (black) when a uniform field of excited fluorophores (dashed black) are exposed to the pulsed STED beam described in Fig. 1. The probability of emitting via spontaneous emission after the STED pulse has completed (red, dashed), and this probability corrected for the decrease in image brightness (red, solid). (c) The PSFs for confocal detection (black), normal STED microscopy (red), or time-gated STED microscopy (blue). Probabilities and PSF were calculated with a STED strength sufficient to produce a 2-fold decrease in the FWHM of the effective PSF compared to the confocal PSF and a STED pulse duration equal to the unstimulated fluorophore lifetime, i.e. $S = 23$ and $t_S = \tau$. All distances are measured in units of the 1/e waist of the electric field of the excitation beam. The T-STED PSF in panel (c) has been corrected for the decrease in image brightness.

2.5 T-STED resolution scaling

To illustrate how the resolution of a pulsed STED measurement is affected by pulses of finite duration, Fig. 3a plots the N-fold decrease in the FWHM of the effective PSF relative to the confocal FWHM as a function of pulse energy for different ratios of pulse duration to un-stimulated fluorophore lifetime ($\alpha = t_S/\tau$). As has been determined previously, the FWHM of the effective PSF decreases roughly as the square-root of the pulse energy, i.e. STED strength [18]. For increased STED pulse duration (i.e. increasing α) the effective PSF shows a similar dependence with STED strength, however, the resolving power of the STED instrument is clearly decreased.

#139954 - $15.00 USD Received 21 Dec 2010; revised 10 Feb 2011; accepted 11 Feb 2011; published 17 Feb 2011

To judge the benefit of time-gating in a pulsed configuration, we determine the percent decrease in the FWHM with time-gating relative to a measurement in which no time-gating is applied for a given STED strength and pulse duration. Figure 3b illustrates that as the STED pulse strength is increased the benefit provided by time-gating also increases though this benefit saturates for large STED strengths. Figure 3c demonstrates that the increase in resolution provided by T-STED also increases with pulse duration with no apparent saturation for long pulses.

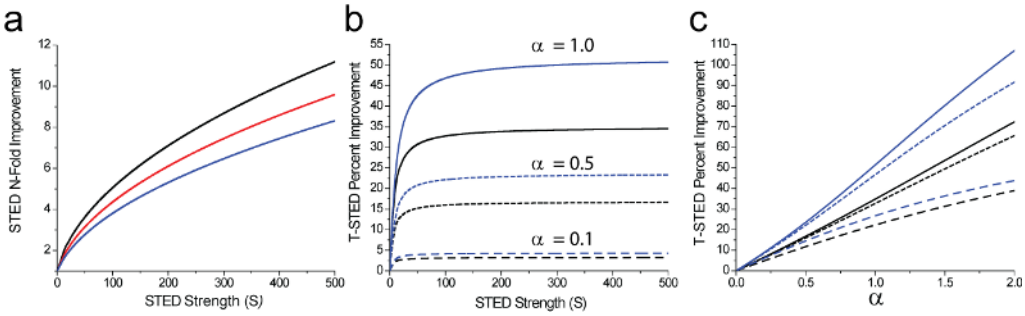

Fig. 3. T-STED Resolution for Pulsed STED. (a) The N-fold increase in the resolving power of a STED microscope over that of a confocal microscope as a function of the strength of the STED beam, *S*. Different pulse durations are plotted in different colors (instant; black; 0.5τ, red; τ, blue.) Increase in resolving power is judged by the relative decrease of the FWHM of the effective PSF from that of the confocal PSF. (b) T-STED resolution improvement over regular STED microscopy judged by the decrease in either the FWHM (black) or the FWQM (blue) for different STED beam strengths. Different pulsed durations are plotted (α = 0.1, large dash; α = 0.5; small dash; and α = 1.0, solid.) (c) Resolution improvement of T-STED over pulsed STED for different α determined with the FWHM (black) or the FWQM (blue). Different STED beam strengths are plotted corresponding to the STED strength required to produce a 2-fold (large dash,) 5-fold (small dash,) or 20-fold (solid) improvement in the FWHM with an instantaneous pulse (black trace in panel a). FWHM and FWQM values were calculated numerically from Eqs. (11) and (18).

Time-gating is a non-linear process; thus, the effect of time-gating will not be a simple rescaling of the spatial extent of the PSF. Rather, the PSF will change shape, with different regions being rescaled to different extents. To estimate this change in the shape, Figs. 3b and 3c also plot the percent improvement in the effective width of the PSF at the full-width-at-quarter-max (FWQM). For all values of the total pulse energy and α, the improvement in the FWQM is always larger than that of the FWHM. Taken together, these results indicate that in addition to a general decrease in the spatial extent of the effective PSF, T-STED also provides a proportionally larger decrease in the spatial extent of the 'tails' of the PSF. Thus, time-gating produces a 'sharper' PSF.

To supplement the numerical results in Fig. 3, we also derive an analytical approximation to the waist of the PSF as a function of the experimental parameters, e.g. pulse duration, fluorophore lifetime, and time-gate. We assume that the final PSF is well-approximated by a Gaussian, $\exp\left(-r^2/\omega_{eff}^2\right)$, with effective waist, ω_{eff}, and expand the natural logarithm of Eq. (17) in a Taylor series around $r=0$. The coefficient of the second order term determines ω_{eff}. We find that the effective beam waist of the T-STED PSF is

$$\omega_{eff}/\omega = \left(4 + S\left(\frac{t_G}{t_S} + \frac{\tau}{t_S}\left(1 - e^{-\frac{t_S}{\tau}\left(1-\frac{t_G}{t_S}\right)}\right)\right)\right)^{-1/2}. \qquad (18)$$

The initial factor of 4 originates from the distinction between the waist of the confocal PSF and that of the electric field of the excitation beam.

Equation (18) simplifies in the absence of the time-gate, yielding

#139954 - $15.00 USD Received 21 Dec 2010; revised 10 Feb 2011; accepted 11 Feb 2011; published 17 Feb 2011

$$\omega_{eff}/\omega = \left(4 + S\frac{\tau}{t_S}\left(1 - e^{-t_S/\tau}\right)\right)^{-1/2}. \quad (19)$$

Either in the limit of an infinitely short STED pulse (with constant STED strength) or of a time-gate equal to the STED pulse duration, Eq. (18) produces the inverse square-root dependence on the STED pulse energy derived previously [18]

$$\omega_{eff}/\omega = \left(4 + S\right)^{-1/2}. \quad (20)$$

Comparison of Eqs. (19) and (20) reveals that the effect of pulses of finite duration is well approximated by decreasing the total STED strength, *S*, by $\frac{\tau}{t_S}\left(1 - e^{t_S/\tau}\right)$. Willig et al. have measured that increasing the STED pulse duration from 200 ps to an effective pulse of ~13 ns with a 3.5 ns fluorophore lifetime requires a ~3.6-fold increase in STED strength to produce the same depletion in the absence of time-gating [16]. Under their experimental conditions, Eq. (19) predicts a ratio of STED strengths of 3.7, in excellent agreement with these measurements.

2.6 T-STED resolution with CW STED beams: theoretically unbounded resolution with finite laser power

In the above discussion, we considered pulsed STED beams; however, STED can also be accomplished with CW beams [16]. Here we expand our discussion to include time-gating with a CW STED source. We assume that the excitation occurs via a pulse with negligible duration and a repetition period, t_E, much larger than the unstimulated fluorophore lifetime, i.e. $t_E >> \tau$. The temporal dynamics for this situation can be derived from the results for a pulsed system, Eq. (5) Section 2.1, in the limit that $t << t_S$ (i.e. $t_S \to \infty$.) In this case, the number of fluorescent photons arriving as a function of time is

$$N_F\left(r,t\right) = n_0 \frac{k}{k + \sigma I\left(r\right)}\left(1 - e^{-\left(k + \sigma I(r)\right)t}\right) \quad (21)$$

and the total number of fluorescent photons is

$$\lim_{t\to\infty} N_F\left(r,t\right) = n_0 \frac{k}{k + \sigma I\left(r\right)}. \quad (22)$$

The spatial dependence in the choice of decay channel, Eq. (22), is what provides the improved resolution in previous demonstration of CW STED [16]. To exploit the additional spatial information encoded in the arrival times, we again propose that the fluorescence signal be time-gated. Fluorescence is collected starting a duration t_G after the completion of the excitation pulse and continues until the beginning of the next excitation pulse. See Fig. 4a. Under the assumption that the excitation pulse repetition period is much larger than the fluorophore lifetime, i.e. $t_E >> \tau$, Eq. (21) produces the time-gated CW STED depletion factor

$$\eta_{CW\,T-STED}\left(r;t_G\right) = \frac{N_F\left(r,\infty\right) - N_F\left(r,t_G\right)}{n_0} = \frac{k}{k + \sigma I\left(r\right)} e^{-kt_G} e^{-\sigma I(r) t_G}. \quad (23)$$

As was observed for the pulsed STED situation above, the final STED depletion factor has both a spatially dependent and independent component. The spatially independent portion, $\exp\left(-kt_G\right)$, represents the decrease in image brightness that occurs with increasing time-

#139954 - $15.00 USD Received 21 Dec 2010; revised 10 Feb 2011; accepted 11 Feb 2011; published 17 Feb 2011

gates. Since this factor applies for all locations, it will not affect the spatial extent of the effective PSF of the microscope. The $I(r)$ terms in both the prefactor and the exponent, on the other hand, will improve the spatial resolution.

Figure 4b illustrates the effect of time-gating with a CW STED beam on the effective PSF of the microscope. When a CW STED beam is applied without time-gating, the width of the effective PSF drops; however, the peak amplitude of the PSF—a measure of the probability of detecting emitted photons—remains constant. Thus, the brightness of a point-emitter will be unchanged. However, when a time-gate is applied, both the width and the maximum amplitude of the effective PSF decrease; thus, a point emitter will appear both sharper and dimmer. To better illustrate the decrease in the spatial extent of the PSF, Fig. 4c plots these same PSFs but normalized to the maximum amplitude. Figures 4d and 4e quantify the decrease in the FWHM with different CW-STED parameters and reveal that increasing either the STED strength or the ratio of the time-gate to the fluorophore lifetime increases resolution.

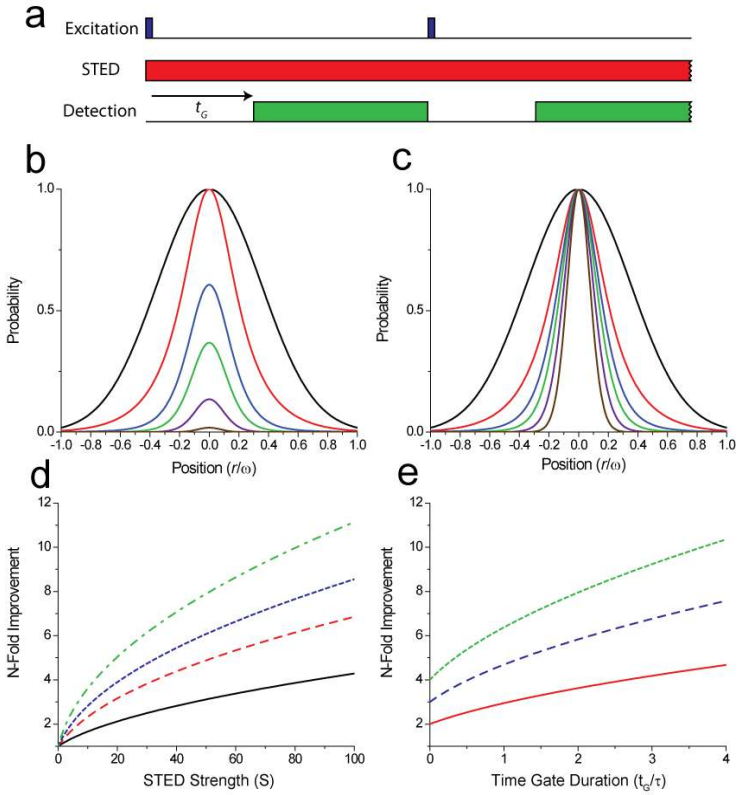

Fig. 4. CW T-STED. (a) Timing diagram for time-gating with a CW STED beam. (b) The effective PSF for different CW T-STED parameters. Plotted are the confocal PSF (black); the effective PSF with a CW STED beam with STED power sufficient to reduce the FWHM to 1/2 that of the confocal PSF (red; $S = \sigma\gamma\omega^2\tau = 16.5$); the same STED beam with $t_G = 0.5\tau$ (blue); $t_G = \tau$ (green); $t_G = 2\tau$ (purple); and $t_G = 4\tau$ (brown). (c) The effective PSF corrected for the decrease in image brightness. The color scheme is the same as in panel (b). (d) The N-fold improvement in the FWHM of the effective PSF with respect to the confocal PSF versus strength of the STED beam. $t_G = 0,1,2,4\tau$ are plotted as solid black, dashed red, dashed blue, and dashed green respectively. (e) The N-fold improvement in the FWHM due to CW T-STED as compared to the confocal PSF versus time-gate duration for different STED beam strengths. Red, blue, and green correspond to STED strengths that decrease the FWHM by 2, 3, and 4-fold in the absence of a time-gate. All distances are measured in units of the 1/e waist of the electric field of the excitation beam. FWHM values were calculated numerically from Eqs. (11) and (23).

#139954 - $15.00 USD Received 21 Dec 2010; revised 10 Feb 2011; accepted 11 Feb 2011; published 17 Feb 2011

As above, we complement the numerical results in Fig. 4 with an analytical estimate for the effective waist of a CW T-STED PSF. We Taylor expand the natural logarithm of the product of the CW T-STED depletion factor, Eq. (23), with the confocal PSF and use the second order coefficient to derive the effective waist

$$\omega_{eff}/\omega = \left(4+\sigma\gamma\omega^2\tau\left(1+t_G/\tau\right)\right)^{-1/2} = \left(4+S'\left(1+t_G/\tau\right)\right)^{-1/2}. \qquad (24)$$

where we slightly modify the STED strength by replacing the pulse duration, undefined for a CW STED beam, with the unstimulated fluorophore lifetime, $S' = \sigma\gamma\omega^2\tau$.

Equation (24) bears a striking similarity to the improvement in spatial resolution derived previously [18] and above, in the limit of an infinitesimally short pulse, Eq. (20). The only distinction is that the effective STED strength is increased by the factor $\left(1+t_G/\tau\right)$ in Eq. (24). Remarkably, the effective STED strength scales linearly with the time-gate duration for a CW T-STED measurement. Since this duration is bounded only by the repetition period of the excitation beam, which can be made as large as desired, the STED strength can be increased arbitrarily simply by increasing the time-gate, without increasing the power of the stimulating beam. In other words, the resolution of a time-gated STED measurement with a CW STED beam is theoretically unbounded for finite laser power. Of course this increase in resolution comes at a price. The prefactor $\exp\left(-kt_G\right)$ implies that images collected with time-gates of increasing duration will be exponentially dimmer.

This result is in sharp contrast to the results derived for a pulsed STED situation, in which time-gating cannot increase the resolution beyond the resolution achieved with an infinitesimally short pulse with the same total energy. The discrepancy between the performance of a pulsed measurement and a CW measurement highlights the physical origin of the increase in resolution: the effective energy of the STED beam. In a pulsed measurement, this energy is fixed by the duration of the pulse, time-gating can only use this energy more effectively, not increase it; thus, resolution is bounded by the resolution achieved with an infinitesimally short pulse. However, in a CW measurement the effective STED energy can be increased simply by integrating the STED beam over larger time-gates, producing increased depletion and increased spatial resolution.

3. Discussion and conclusions

In this Letter, we solve a simple kinetic model for the temporal dynamics of excited fluorophores in the presence of a spatially varying stimulating beam of variable duration and demonstrate that spatial information is contained in the arrival times of the spontaneous emission. To extract this extra information, we propose that the fluorescence signal should be time-gated, and we derive the increase in spatial resolution provided by time-gating for both pulsed and CW STED beams. In both cases, time-gating provides higher resolution but dimmer images.

When might T-STED be a useful alternative to a STED measurement? The lifetimes of the fluorophores useful for STED measurements range from 100s of ps to a few ns. STED pulse durations, on the other hand, range from 10s of ps [19] to ~1 ns [20]. Thus, for pulsed STED measurements, the range of α values is large, ~0.01 - 10. For measurements, with small α values, <0.5, the resolution enhancement provided by time-gating will likely be negligible. In fact, the improvement may be so modest that it is not measurable—an observation that may explain why a change in STED depletion as a function of pulse duration was not observed in a previous study [21]. However, for larger α values, the improvement in resolution is significant, and these measurements will likely benefit from time-gating.

Interestingly, the benefits of time-gating in a pulsed STED measurement are not limited to improved resolution. First, as has been widely recognized, time-gating can remove stray scattered light from the STED beam not removed by filters, decreasing background noise significantly in some situations. However, beyond this concern, we have now revealed that

#139954 - $15.00 USD Received 21 Dec 2010; revised 10 Feb 2011; accepted 11 Feb 2011; published 17 Feb 2011

pulse durations can be increased, with no loss in resolution, when time-gating is applied. The ability to spread the pulse power over longer durations, decreasing the instantaneous intensity of the pulse, may allow experimentalists to avoid known issues such as inefficient depletion during vibrational relaxation [17] and STED intensity-dependent photobleaching [21]. STED measurements are often limited by the photostability of current dyes; thus, the ability to reduce photobleaching through longer pulses with no loss in resolution is an important additional benefit of T-STED.

The major benefit of T-STED with a CW laser source will likely be the ability to increase resolution significantly without the use of additional laser power. However, it is important to note that while, in theory, the resolution of a CW TSTED measurement is unbounded. In practice, there will likely be a maximum resolution given the specific STED laser, the fluorophore lifetime and photostability, and the background noise of the measurement. Image resolution increases slowly with the time-gate duration—as the square-root—while the brightness decreases exponentially. Thus, there will be a maximum time-gate beyond which the image will not be bright enough to be distinguished from background noise, and this maximum time-gate will set the maximum image resolution. To surpass this practical limit additional laser power will be needed. Alternatively, our analysis reveals that an increase in the resolution can also be produced by using fluorophores with longer lifetimes. This observation makes color centers in diamond all the more exciting as STED probes since these fluorophores have particularly long lifetimes, >10 ns [13,22]. Thus, through the simple addition of a time-gate, it may be possible to significantly increase the 6 nm resolution recently reported with CW-STED imaging of color centers [13].

While our discussion here has focused on a measurement in which all fluorescence before a certain period is discarded, practical implementations of T-STED will likely collect all fluorescence and record arrival times using time correlated photon counting hardware. In fact, such a time-resolved STED instrument has already been created and used to perform lifetime imaging in a pulsed STED setting. Initial observations [23] support the increase in resolution with time-gating we describe here. The advantage of measuring the arrival time of all photons, particularly for CW T-STED, is that time-gating can be applied in offline analysis, allowing the experimentalist to dynamically adjust the balance between resolution and image brightness to meet the demands of the specific application.

It was long thought that the resolution of far-field optics was fundamentally limited by diffraction, but it is now clear that a variety of techniques can embed additional spatial information in the optical measurement and leverage this additional information to image spatial features well below the diffraction limit. Here we show that minor differences in fluorescence lifetimes, created by differences in the local intensity of the STED beam, can be amplified into measureable differences in arrival times, revealing that the last photons to arrive carry the most spatial information. The construction of microscopes to extract this extra information should help push the practical limits of far-field imaging even further beyond the diffraction limit.

#139954 - $15.00 USD Received 21 Dec 2010; revised 10 Feb 2011; accepted 11 Feb 2011; published 17 Feb 2011